

1 *Revised on 11-25-2008 after “pre-edit Bao2” by editor*

2 **Stretching the envelope of past surface environments: Neoproterozoic glacial lakes**  
3 **from Svalbard**

4  
5 Huiming Bao<sup>1</sup>, Ian J. Fairchild<sup>2</sup>, Peter M. Wynn<sup>3</sup> & Christoph Spötl<sup>4</sup>

6  
7  
8 <sup>1</sup>*Department of Geology & Geophysics, E235 Howe-Russell Complex, Louisiana State*  
9 *University, Baton Rouge, LA 70803, USA. <sup>2</sup>School of Geography, Earth and*

10 *Environmental Sciences, University of Birmingham, Birmingham B15 2TT, UK.*

11 <sup>3</sup>*Department of Geography, University of Lancaster, Lancaster, LA1 4YQ, UK Lancaster*  
12 *University, UK. <sup>4</sup>Institut für Geologie und Paläontologie, Leopold-Franzens-Universität*

13 *Innsbruck, Innrain 52, 6020 Innsbruck, Austria*

14

15 **One-sentence summaries:**

16 Extreme multi-stable isotope compositions of sulfate and its host carbonates from  
17 Svalbard reveal an extraordinary atmosphere-biosphere condition during the deposition  
18 of a Neoproterozoic glacial diamictites.

19

20 **Abstract**

21 **The oxygen isotope composition of terrestrial sulfate is affected measurably by**  
22 **many Earth surface processes. During the Neoproterozoic, severe “Snowball”**  
23 **glaciations would have had an extreme impact on the biosphere and the atmosphere.**  
24 **Here, we report that sulfate extracted from carbonate lenses within a**  
25 **Neoproterozoic glacial diamictite suite from Svalbard, with an age of ~ 635 Ma, falls**  
26 **well outside the currently known natural range of triple oxygen isotope**  
27 **compositions, and indicates that the atmosphere had either an exceptionally high**  
28 **atmospheric CO<sub>2</sub> concentrations or an utterly unfamiliar O<sub>2</sub> cycle during deposition**  
29 **of the diamictites.**

30 Terrestrial sulfate ( $\text{SO}_4^{2-}$ ) has diverse origins and participates in many important  
31 physicochemical and biological processes that can be inferred from large ranges in stable  
32 sulfur and oxygen isotope compositions (1). The  $\delta^{18}\text{O}$  (2) of sulfate ranges from  $\sim+8\text{‰}$  to  
33  $\sim+27\text{‰}$  (VSMOW) (3) for marine sulfate of different geological ages (4) and down to  
34  $\sim-18\text{‰}$  for sulfate formed in continental Antarctica (5). In recent years, the sulfate  
35 oxygen isotope composition has been found to vary along another dimension, the  $\Delta^{17}\text{O}$  [ $\equiv$   
36  $\ln(\delta^{17}\text{O}+1) - 0.52\ln(\delta^{18}\text{O}+1)$ ]. The  $\Delta^{17}\text{O}$  is close to zero for most samples, but positive  
37 (up to  $\sim+5.94\text{‰}$ ) for those of atmospheric origin (6, 7). Most recently, small but negative  
38  $\Delta^{17}\text{O}$  values have been reported for sulfate derived from oxidative weathering by  
39 atmospheric oxygen, with a conspicuous spike (down to  $-0.70\text{‰}$ ) in the immediate  
40 aftermath of a Marinoan glaciation at  $\sim 635$  Myrs ago (8). Here we report that these  
41 ranges are surpassed dramatically by carbonate-associated sulfate (CAS) extracted from a  
42 Neoproterozoic Marinoan (9, 10) carbonate unit from Svalbard, Arctic Ocean. This  
43 carbonate member (W2) is from the Wilsonbreen Formation (Polarisbreen Group), a  
44 formation dominated by diamictites representing a continental-scale glaciation (ref. 9, 11).  
45 W2 contains both limestones and primary dolostones with exceptionally preserved  
46 geochemistry (12). We have greatly extended the previous geochemical database,  
47 including isotope compositions of CAS (13) (Fig. S1, Table S1). Note that the “cap  
48 carbonate”, the lower Dracoisen Formation, is  $\sim 80$  m above W2, and is not the subject of  
49 this study.

50 Two features of the dataset are exceptional in terms of what we know about sulfate  
51 on Earth (Fig. 1): 1) The  $\Delta^{17}\text{O}_{\text{CAS}}$  reaches as low as  $-1.64\text{‰}$ , the most negative anomaly  
52 ever reported for terrestrial (vs. extraterrestrial) minerals; 2) The  $\delta^{18}\text{O}_{\text{CAS}}$  reaches as high

53 as  $\sim +37.7\%$ , the most positive value ever reported for natural sulfate oxygen. Additional  
54 features are also intriguing. For example: 3) CAS with a distinct  $^{17}\text{O}$  anomaly is  
55 invariably from a limestone phase whilst CAS from the dolostone phase does not have  
56 such a distinct  $^{17}\text{O}$  anomaly (Fig. 1); 4) Amongst CAS from the limestones, there is a  
57 strong positive correlation in  $\Delta^{17}\text{O}-\delta^{34}\text{S}$  space and the trend line connects with CAS from  
58 the immediately pre-glacial dolostone (member E4) (Fig. 1b); 5) The positively  
59 correlated  $\delta^{18}\text{O}$  and  $\delta^{13}\text{C}$  of dolomite ranges from  $\sim -11\%$  to  $+15\%$  (VPDB) (3) and from  
60  $\sim -2$  to  $+5\%$  (VPDB) respectively. This  $\delta^{18}\text{O}_{\text{CO}_3}$  is the most positive value ever reported  
61 (Fig. 2a); 6) Excluding pre-glacial samples, a slope of  $\sim 1$  links two clusters of data in  
62  $\delta^{18}\text{O}_{\text{CAS}} - \delta^{18}\text{O}_{\text{CO}_3}$  space (Fig. 3); and 7) those calcite samples with negative  $\Delta^{17}\text{O}_{\text{CAS}}$   
63 have a  $\Delta^{17}\text{O}_{\text{CO}_3}$  value close to zero, indicating the evaporated water itself did not bear a  
64  $^{17}\text{O}$  anomaly (Table S1).

65 We propose the following model to account for this unusual carbonate paragenesis.  
66 The environment consisted of lacustrine oases within a continental ice sheet. The lakes  
67 were dominantly suboxic and, where local meltwater inflow was low, they and their near-  
68 surface porewaters were driven to high salinities by extreme evaporation, accompanied  
69 by intense microbial sulfate redox reactions. Sulfate with negative  $\Delta^{17}\text{O}$  values was  
70 produced by oxidative weathering involving atmospheric  $\text{O}_2$  on the land surface, and was  
71 washed into the lakes, along with pre-existing sulfate in rocks undergoing weathering.  
72 This mixed sulfate was reduced to sulfides ( $\text{H}_2\text{S}$  or  $\text{HS}^-$ ) by bacteria and subsequently  
73 reoxidized to sulfate by a different microbial community in an oxic to suboxic condition.  
74 The re-oxidation was highly efficient, thus causing sulfur isotope mass-balance and  
75 resulting in a change in the  $\delta^{34}\text{S}_{\text{SO}_4}$  much smaller than in the corresponding  $\delta^{18}\text{O}_{\text{SO}_4}$  or

76  $\delta^{18}\text{O}_{\text{CO}_3}$  value (which should be heavily influenced by the changing  $\delta^{18}\text{O}_{\text{H}_2\text{O}}$  due to  
77 variable degrees of evaporation). No atmospheric  $\text{O}_2$  signal was incorporated into the  
78 newly regenerated sulfate in the water column, as abundant Mn and Fe (Table S1) would  
79 shuttle electrons between sulfite and dissolved  $\text{O}_2$  in ambient solution (14-16) without  
80 direct contact between reduced sulfur species and  $\text{O}_2$ . Such redox cycling effectively  
81 eliminated the initial sulfate  $^{17}\text{O}$ -anomalous oxygen and replaced it with  $^{17}\text{O}$ -normal  
82 oxygen from the ambient water during the precipitation of dolostones. The sulfate in  
83 limestones however appears not to have been subjected to such intense redox cycling,  
84 thus enabling them to retain their  $^{17}\text{O}$ -anomalous signature. Intensive evaporation  
85 resulted in highly positive  $\delta^{18}\text{O}$  values for the remaining water in a restricted lake or  
86 basin. Carbonate formed in the water would also therefore carry extremely positive  $\delta^{18}\text{O}$   
87 values. Both the dolomite mineralogy and the ranges of  $\delta^{13}\text{C}_{\text{CO}_3}$  and  $\delta^{18}\text{O}_{\text{CO}_3}$  (displaying  
88 heavier-than-marine values) are characteristic of restricted evaporitic settings (17).

89       The evaporative dolomite-precipitating environments are evidence of microbial  
90 activity because they contain microbial laminites (12) and due to the intense redox  
91 cycling required to explain both the extremely high  $\delta^{18}\text{O}_{\text{CAS}}$  values and the disappearance  
92 of the negative  $^{17}\text{O}$  anomalies in these dolomites. As  $\delta^{18}\text{O}_{\text{CAS}}$  increases at the same  
93 magnitude as  $\delta^{18}\text{O}_{\text{CO}_3}$  (Fig. 3), this suggests that almost all the oxygen in the sulfate was  
94 replaced by oxygen from ambient water after microbially-mediated sulfur redox cycling.  
95 The highly positive  $\delta^{18}\text{O}_{\text{SO}_4}$  (up to +37.7‰) therefore should be correlated with the  
96 highly positive  $\delta^{18}\text{O}_{\text{H}_2\text{O}}$  in the lakes. The  $\delta^{18}\text{O}$  of evaporated  $\text{H}_2\text{O}$  can be estimated from  
97 the highly positive  $\delta^{18}\text{O}_{\text{dolomite}}$ , which is unlikely the result of late alteration. Taking into  
98 account the uncertainties in precipitation temperature, precipitation kinetics, and

99 diagenetic imprint, we estimate (from Fig. 3) a difference between  $\delta^{18}\text{O}_{\text{CAS}}$  and  $\delta^{18}\text{O}_{\text{H}_2\text{O}}$   
100 ranging from  $\sim 20\text{‰}$  to  $30\text{‰}$ , which is similar to the  $\sim 25\text{‰}$  to  $30\text{‰}$  recently obtained  
101 from an experimental studies of sulfate reduction (18). We know of no other  
102 environments where the microbial sulfate redox cycling has reached a complete steady  
103 state with highly evaporitic ambient water. The closest analog is modern hypersaline  
104 lagoons near Rio de Janeiro, Brazil, where the  $\delta^{18}\text{O}_{\text{SO}_4}$  reaches  $+21.3\text{‰}$  in pore waters  
105 and  $+20.8\text{‰}$  in surface brines with an apparent  $\Delta\delta^{18}\text{O}_{\text{SO}_4-\text{H}_2\text{O}}$  at  $\sim +20\text{‰}$  (19).

106 The most negative value of  $\Delta^{17}\text{O}_{\text{SO}_4}$  ( $-1.64\text{‰}$ ) extends greatly the magnitude and  
107 geographic occurrence of the negative  $\Delta^{17}\text{O}_{\text{SO}_4}$  following the Marinoan glaciation as first  
108 reported in Bao et al. (8). Bao et al proposed the negative  $\Delta^{17}\text{O}$  was derived from that of  
109 atmospheric  $\text{O}_2$  involved in the oxidative weathering of sulfur compounds on the surface  
110 of the Earth (8). Pre-existing ocean sulfate may not have a distinct negative  $\Delta^{17}\text{O}$  value  
111 because continuous microbial sulfur redox cycling tends to replace sulfate oxygen with a  
112 water oxygen signal. Thus, sulfate in a restricted continental basin could have the most  
113 negative  $\Delta^{17}\text{O}_{\text{SO}_4}$  where a significant portion of the sulfate was derived from non-marine  
114 sources. The value  $-1.64\text{‰}$  is more than twice the magnitude of the  $-0.70\text{‰}$  reported for  
115 barites from Marinoan cap carbonates from South China (8). This is consistent with W2's  
116 setting, where much if not all the drainage could have been internal.

117 We interpret the strong correlation between  $\Delta^{17}\text{O}_{\text{CAS}}$  and  $\delta^{34}\text{S}_{\text{CAS}}$  in limestones (data  
118 feature 4, Fig. 1b) as a mixing line between two sulfate endmembers: a pre-existing  
119 marine sulfate and a sulfate newly supplied from continental weathering, rather than an  
120 evaporative trend for an already mixed sulfate in the lakes. This can be justified because  
121 of the absence of evaporative characteristics in the limestones and their much narrower

122 scatter of  $\delta^{18}\text{O}$  value (from  $-13\text{‰}$  to  $-4\text{‰}$ VPDB) (Fig. 2b, Fig. 3) compared with that of  
123 the evaporative dolomites (from  $-11\text{‰}$  to  $+15\text{‰}$ VPDB) (Fig. 2a). The “mixing” scenario  
124 is also supported by the isotope compositions of CAS in the pre-glacial carbonates, which  
125 fall close to the  $\delta^{34}\text{S}$ -high end of the line (Fig. 1b). Since sulfate evaporite relics are  
126 known to occur in the underlying E4 tidal-flat carbonates (20) it is likely that weathering  
127 of coeval nodular or bedded sulfate from lateral equivalents of E4 helped stabilize the  
128 position of the mixing line.

129         If sulfate derived from oxidative weathering of sulfides in glacial rock flour had a  
130 global average crustal  $\delta^{34}\text{S}$  value of  $\sim 0\text{‰}$ , the mixing line (Fig. 1b) would point to a  
131  $\Delta^{17}\text{O}$  of  $\sim -4.2\text{‰}$  for the non-marine sulfate endmember. This would imply an  
132 atmospheric  $\Delta^{17}\text{O}(\text{O}_2)$  at  $\sim -42\text{‰}$  if only 10% of the oxygen in sulfate came from  
133 atmospheric  $\text{O}_2$  (8). This estimate contains two large uncertainties – the end-member  
134  $\delta^{34}\text{S}_{\text{sulfides}}$  value and the fraction of sulfate oxygen derived from atmospheric  $\text{O}_2$  – and is  
135 likely the most negative bound. If the non-marine sulfate endmember had a  $\delta^{34}\text{S}$  of  $\sim$   
136  $+18\text{‰}$ , as seen near the low end of the data array (Fig. 1b), the atmospheric  $\Delta^{17}\text{O}(\text{O}_2)$   
137 would be  $\sim -6.6\text{‰}$  assuming 1/4 of the oxygen in sulfate (a probable maximum) came  
138 from atmospheric  $\text{O}_2$  during surface sulfide oxidation (16, 21). A realistic  $\Delta^{17}\text{O}(\text{O}_2)$  value  
139 probably lies somewhere between  $-42\text{‰}$  and  $-6.6\text{‰}$  at the time of W2 deposition. Note  
140 that the modern  $\Delta^{17}\text{O}(\text{O}_2)$  is only  $\sim -0.10$  to  $-0.20\text{‰}$  depending on reference slope value  
141  $(\ln\alpha^{17}/\ln\alpha^{18})$  used for calculation (22, 23).

142         There may be alternative scenarios where a large negative  $\Delta^{17}\text{O}(\text{O}_2)$  could occur  
143 mathematically, although geologically there are far fewer scenarios that are viable. The  
144 magnitude of the negative  $\Delta^{17}\text{O}$  value of atmospheric  $\text{O}_2$  is determined by parameters

145 such as stratosphere O<sub>3</sub>-CO<sub>2</sub>-O<sub>2</sub> reactions, the size of the atmospheric O<sub>2</sub> and CO<sub>2</sub>  
146 reservoirs, stratosphere-troposphere flux, and troposphere O<sub>2</sub> fluxes (8). The controlling  
147 parameters are often hard to determine, especially for an unfamiliar Earth system, but  
148 some constraints exist. Other things being equal, higher CO<sub>2</sub> concentrations lead to a  
149 more negative  $\Delta^{17}\text{O}(\text{O}_2)$  value as the CO<sub>2</sub> develops a positive anomaly by exchange with  
150 oxygen. Assuming a steady-state O<sub>2</sub> reservoir and modern gas fluxes, the 1-D model in  
151 Bao et al (8) would predict a pCO<sub>2</sub> level of ~12,500 to ~ 80,000 ppm during W2  
152 deposition, consistent with the Earth having gone through a prolonged, ice-covered  
153 period, i.e. a ‘snowball’ Earth (24). It should be noted that a much lower pO<sub>2</sub> and a  
154 moderately high pCO<sub>2</sub> also could produce a similarly negative  $\Delta^{17}\text{O}(\text{O}_2)$ , but only if the  
155 corresponding O<sub>2</sub> residence time (i.e. pO<sub>2</sub>/flux) were disproportionately long. Prolongation  
156 of the residence time whilst keeping oxygen concentrations low implies much lower rates  
157 of both O<sub>2</sub> removal by respiration/decomposition and input by photosynthesis, a balance  
158 that is consistent with near-global glaciations. Other non-steady-state scenarios can also  
159 be imagined where bizarre combinations of changes in reservoirs and fluxes of  
160 atmospheric O<sub>2</sub> and CO<sub>2</sub> could have resulted in the observed large negative  $\Delta^{17}\text{O}(\text{O}_2)$  in  
161 certain time windows. These scenarios could be explored by combining models and  
162 further empirical data, but geology offers a stronger constraint since circumstances under  
163 which sulfate can be preserved in terrestrial sedimentary records are uncommon.

164       Although various aspects of Neoproterozoic glaciations are intensely disputed (25),  
165 our results confirm a profound difference from Phanerozoic ice ages. A near-global  
166 distribution of glaciated continents during a ‘Marinoan’ phase ending 635-630 Myr ago is  
167 supported by evidence of low palaeomagnetic latitudes (26). The ‘snowball’ Earth model

168 (27) predicts a progressive accumulation of volcanic volatiles in the atmosphere which  
169 are not removed by weathering until the rapid demise of the ice age as the ice-albedo  
170 feedback reverses. If sulfate with large negative  $\Delta^{17}\text{O}$  signals derived from oxidative  
171 weathering could only be generated in significant quantity after melting of the “snowball”  
172 and exposure of continents, then the diamictites above W2 had to be deposited during  
173 final glacial retreat, a hypothesis that should prompt a re-examination of their  
174 sedimentology. The alternative “slushball” model, in which parts of the ocean area are  
175 ice-free (28), would also permit accumulation of sulfate from prolonged oxidative  
176 weathering in certain continental “oases” where arid but cold conditions prevailed. This  
177 study provides an effective way to study the dynamics of sedimentation and atmospheric-  
178 hydrosphere-biosphere interactions during a global glaciation and highlights the need for  
179 further stratigraphically constrained  $\Delta^{17}\text{O}_{\text{SO}_4}$  data on continental carbonate precipitates to  
180 ground-truth flux-balance models.

181



182 **References and Notes**

- 183 1. H. M. Bao, D. Rumble, D. R. Lowe, *Geochimica et Cosmochimica Acta* 71, 4868  
184 (2007).
- 185 2.  $\delta^{18}\text{O}$  or  $\delta^{17}\text{O} \equiv R^x_{\text{sample}}/R^x_{\text{standard}} - 1$  and  $R^x = {}^{18}\text{O}/{}^{16}\text{O}$  or  ${}^{17}\text{O}/{}^{16}\text{O}$ ; the same  $\delta$   
186 notation applies to  $\delta^{13}\text{C}$  or  $\delta^{34}\text{S}$  in this paper.
- 187 3. Reference units for stable isotope compositions: Vienna Standard Mean Ocean  
188 Water (VSMOW) for sulfate  $\delta^{18}\text{O}$ ,  $\delta^{17}\text{O}$ , and  $\Delta^{17}\text{O}$ , Vienna PeeDee Belemnite  
189 (VPDB) for carbonate  $\delta^{13}\text{C}$  and  $\delta^{18}\text{O}$ , and Vienna Canyon Diablo Troilite (VCDT)  
190 for sulfate  $\delta^{34}\text{S}$ .
- 191 4. G. E. Claypool, W. T. Holser, I. R. Kaplan, H. Sakai, I. Zak, *Chemical Geology*  
192 28, 199 (1980).
- 193 5. R. A. Socki, R. P. Harvey, D. L. Bish, E. Tonui, H. Bao, in *Lunar and Planetary*  
194 *Science Conference*. (NASA, Houston, 2008), vol. XXXIX, pp. 1964.
- 195 6. H. M. Bao, *Chemical Geology* 214, 127 (2005).
- 196 7. H. M. Bao, M. H. Thiemens, D. B. Loope, X. L. Yuan, *Geophysical Research*  
197 *Letters* 30, 1843; 10.1029/2003GL016869 (2003).
- 198 8. H. M. Bao, J. R. Lyons, C. M. Zhou, *Nature* 453, 504 (2008).
- 199 9. G. P. Halverson, A. C. Maloof, P. F. Hoffman, *Basin Research* 16, 297 (2004).
- 200 10. G. P. Halverson, in *Neoproterozoic Geobiology and Paleobiology* S. Xiao, A. J.  
201 Kaufman, Eds. (Springer, New York, 2006) pp. 231-271.
- 202 11. I. J. Fairchild, M. J. Hambrey, *Precambrian Research* 73, 217 (1995).
- 203 12. I. J. Fairchild, M. J. Hambrey, B. Spiro, T. H. Jefferson, *Geological Magazine*  
204 126, 469 (1989).

- 205 13. Materials and methods are available as supporting material on *Science Online*.
- 206 14. G. W. Luther, *Geochimica et Cosmochimica Acta* 51, 3193 (1987).
- 207 15. C. O. Moses, J. S. Herman, *Geochimica et Cosmochimica Acta* 55, 471 (1991).
- 208 16. N. Balci, W. C. Shanks, B. Mayer, K. W. Mandernack, *Geochimica et*  
209 *Cosmochimica Acta* 71, 3796 (2007).
- 210 17. M. R. Talbot, *Chemical Geology* 80, 261 (1990).
- 211 18. J. Farquhar, D. E. Canfield, A. Masterson, H. Bao, D. Johnston, *Geochimica et*  
212 *Cosmochimica Acta* 72, 2805 (2008).
- 213 19. N. F. Moreira, L. M. Walter, C. Vasconcelos, J. A. McKenzie, P. J. McCall,  
214 *Geology* 32, 701 (2004).
- 215 20. I. J. Fairchild, M. J. Hambrey, *Precambrian Research* 26, 111 (1984).
- 216 21. B. J. Reedy, J. K. Beattie, R. T. Lowson, *Applied Spectroscopy* 48, 691 (1994).
- 217 22. A. Angert, S. Rachmilevitch, E. Barkan, B. Luz, *Global Biogeochemical Cycles*  
218 17, #1030 (2003).
- 219 23. B. Luz, E. Barkan, *Geochimica et Cosmochimica Acta* 69, 1099 (2005).
- 220 24. R. T. Pierrehumbert, *Journal of Geophysical Research-Atmospheres* 110 (2005).
- 221 25. I. J. Fairchild, M. J. Kennedy, *Journal of the Geological Society* 164, 895 (2007).
- 222 26. D. A. D. Evans, *American Journal of Science* 300, 347 (2000).
- 223 27. P. F. Hoffman, D. P. Schrag, *Terra Nova* 14, 129 (2002).
- 224 28. T. J. Crowley, W. T. Hyde, W. R. Peltier, *Geophysical Research Letters* 28, 283  
225 (2001).
- 226
- 227

228 29. H.B. and I.J.F. designed research and led the writing of the manuscript. H.B.  
229 performed CAS extraction and triple oxygen isotope measurements. I.J.F secured  
230 samples from field expeditions, and conducted sedimentological, petrographic,  
231 mineralogical and elemental studies. P.M.W. conducted preliminary CAS  
232 extraction and performed  $\delta^{34}\text{S}_{\text{CAS}}$  analysis; C.S. carried out  $\delta^{13}\text{C}$  and  $\delta^{18}\text{O}$  analysis  
233 of host carbonates. We thank Galen Halverson for discussion and Yongbo Peng  
234 for analytical assistance. Financial and facility supports are provided by LSU,  
235 NSF, and Chinese Academy of Science (H.B.), NERC standard grant  
236 (GR3/C511805/1) and NERC ICP-MS facilities (I.J.F.), and Austrian Science  
237 Funds (C.S.).

238

### 239 **Author Information**

240 The authors declare no competing financial interests.

241 Correspondence should be addressed to H.B. ([bao@lsu.edu](mailto:bao@lsu.edu)).

242

### 243 **Figures;**

244

245

246

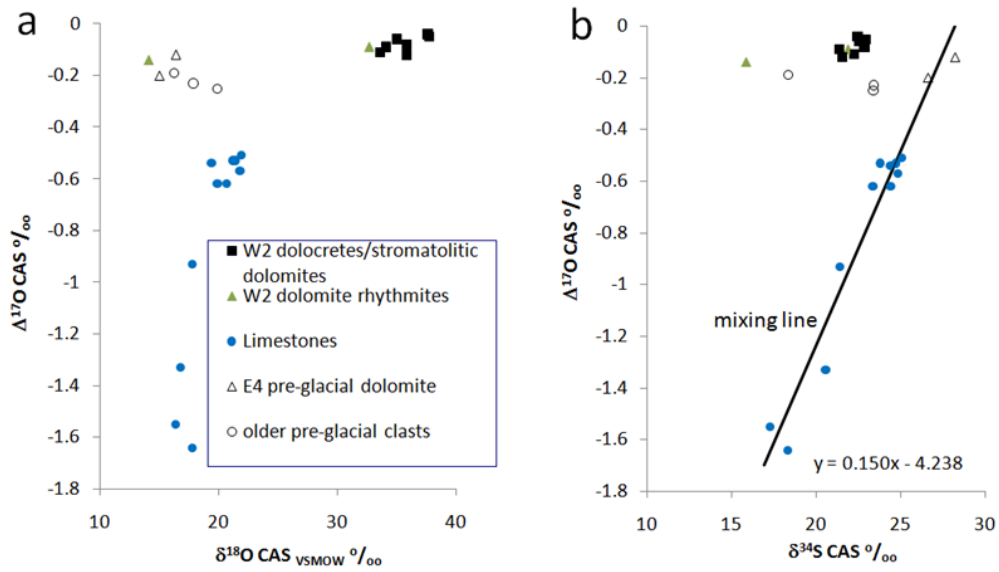
247

248

249

250

251 **Figure 1**

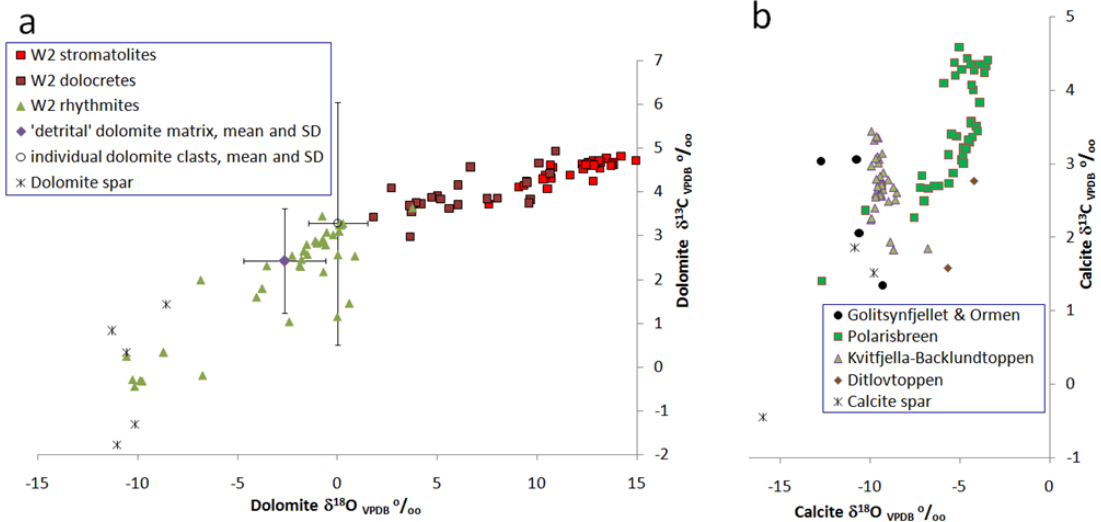


252

253

254

255 **Figure 2**



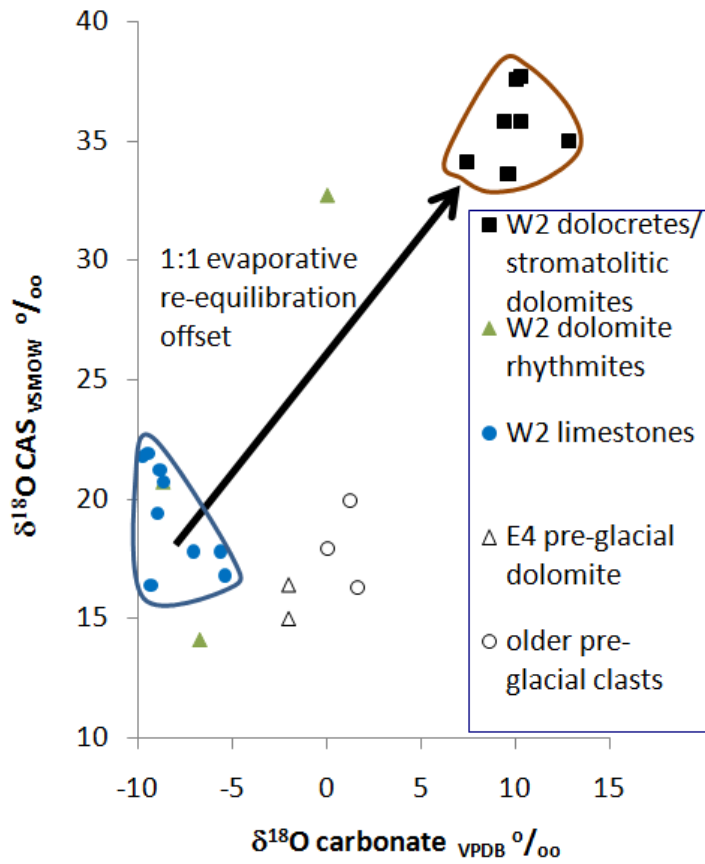
256

257

258

259 **Figure 3**

260



261

262

263

264

265

266

267

268

269

270 **Supporting Online Material**

271 1. Methods

272 2. The Middle Carbonate Member (W2) the Wilsonbreen Formation, Neoproterozoic

273 Svalbard

274 Table S1

275 Table S2

276

277